

CHAPTER 5

Ultra-Low Voltage FTM transferred DPP-DTT Based Near Infra-Red Phototransistor*.

*Part of this work has been under revision in IEEE transaction of electron devices

Prashant Kumar, V. N. Mishra, and R. Prakash, “Ultra-Low Voltage FTM transferred DPP-DTT Based Near Infra-Red Phototransistor,” *IEEE Electron devices (under review)*.

CHAPTER 5

Ultra-Low Voltage FTM transferred DPP-DTT Based Near Infra-Red Phototransistor.

5.1 Introduction

Near Infrared photodetectors find their applications in remote sensing of parameters like temperature, environmental monitoring, thermal efficiency analysis, and night vision. Organic semiconductors are better alternatives to inorganic NIR photodetectors because of their easy and low-cost solution processability and compatibility with flexible substrates and large area electronics[58], [62], [119]. Broadly Organic photodetectors can be classified as Photo conductors, p-n junction-based photodiodes, and Organic Field effect-based Phototransistors. In Comparison to photodiodes, OPTs consist of the third electrode (gate electrode) which provides an additional control to change the sensitivity of the device by varying gate voltage. Moreover, the three-terminal configuration of OPTs helps in designing the active matrix-type sensing arrays which are necessary building blocks of the practical two-dimensional photodetectors[56], [62], [120], [121]. Even though NIR photodetectors can find their application in thermal imaging, biomedical monitoring systems, and night vision comparatively little attention has been given to NIR OPTs with respect to visible OPTs. Furthermore, most of the reported OPTs are working in the voltage range of -5 to -50 V making them unsuitable for portable and wearable devices[56], [58]–[60], [62], [120]. Additionally, after COVID-19 pandemic the home assisted and portable medical diagnostic kits for applications like pulse oximetry and monitoring of blood pressure are in demand where red

and NIR regions provide maximum contrast for absorption of oxyhemoglobin and hemoglobin which results in higher detection accuracy and selectivity. Most of these devices work by detecting the flow of blood in tissues. This further establishes that more focus on ultra-low power NIR OPTs is needed[122]. The use of a high k dielectric can lower the operating voltage. Organic dielectrics like Polyvinyl Alcohol (PVA), poly(4-vinyl phenol) (PVP), and Poly(vinylidene fluoride) (PVDF) have been extensively used to lower operating voltage because of their high k values. Another advantage of organic high k dielectrics is they can be easily adapted for flexible substrates and provide a better interface for organic semiconductors. PVA (chemical formula depicted in Fig. 5.1 (e)) is a high k organic dielectric that can be easily processed through water, suitable for low temperature processing, and biocompatible too[120], [123], [124]. So, we have selected it as the dielectric layer.

Among solution process techniques for the organic semiconductor (OSC) layer, the Floating film transfer method (FTM) is highly suitable for large area processing with additional benefits like no requirement of costly and bulky instruments, and minimal wastage of OSC solution thereby making it a cost-effective method. FTM is a better option than spin coating because it stamps a preexisting self-assembled floating film, as opposed to spin coating, which can result in the solution-processed organic dielectric layer dissolution without the use of orthogonal solvent[77], [86]. Charge trapping at dielectric interface is generally considered a negative process hindering the device performance[4]. This interesting phenomenon arising at dielectric semiconductor interface has been used to improve the performance of OPTs. However the reported OPTs with charge trapping phenomenon are working at comparatively higher voltages or are using costlier methods of semiconductor deposition (like vapor deposition) or methods

like spin coating which are not suitable for large area electronics thereby hindering the portability and making the process unsuitable for large area electronics[125]–[128]. Here we combine the charge trapping phenomenon at the semiconductor dielectric interface and large area and low-cost processing advantages of FTM method using eco-friendly water as liquid substrate to fabricate high performance OPTs.

DPP-DTT (chemical structure shown in 1(c)), with the highest occupied molecular orbital (HOMO) and lowest unoccupied molecular orbital LUMO levels of ~ -5.5 eV and ~ -3.9 eV was selected for the active layer. This is suitable for NIR phototransistors because of its smaller bandgap of ~ 1.7 eV[97]. In this report, we have utilized the water processed organic dielectric PVA without any crosslinking agent as the dielectric layer and DPP-DTT as the OSC layer. The FTM film is transferred from the surface of the water. The Fabricated device (Schematic, image, and SEM image of which is shown in Fig. 5.1 (a), (b), and (d) respectively) has shown ultra-low voltage operation with very small dark current due to charge traps on the surface of PVA dielectric. The PVA/DPP-DTT phototransistor shows power sensitivity (P) of ~ 456 responsivity (R) of ~ 7.72 A/W, external quantum efficiency (EQE) of ~ 1183.84 %, and detectivity of $\sim 1.097 \times 10^{12}$ Jones. Since the maximum temperature for processing is not more than 100°C , this device is highly suitable for implementation on flexible substrates. This chapter is organized in five sections including this. The 5.2 section covers experimental details followed by the characterization details in section 5.3. The 5.4 section includes the results of electrical and optical measurement followed by conclusion in 5.5 section.

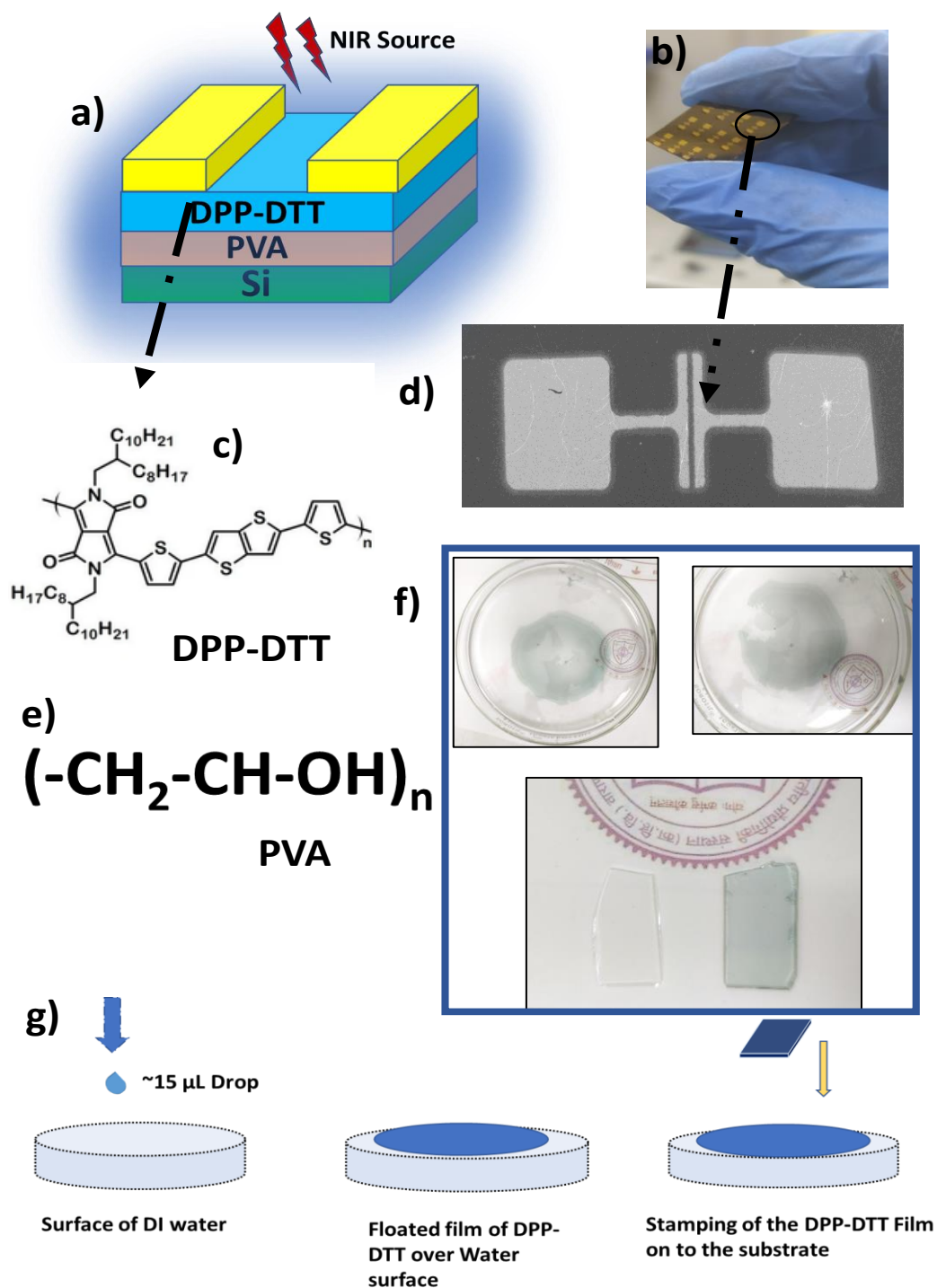


Fig. 5.1. (a) Schematics of the Fabricated Device, (b) Image of the Device (c) Chemical Structure of DPP-DDT polymer (d) SEM image of the channel (e) Chemical Structure of Polyvinyl Alcohol, (f) Processed FTM film of DPP-DDT over DI water surface (g) steps involved in FTM process.

5.2 Experimental Details and Device Fabrication Steps

5.2.1 Material Details: Ossila Ltd. UK supplied the DPP-DTT compound with a molecular weight of ~ 100,000 while Sigma Aldrich delivered chemicals including PVA (Mw. ~98000), chloroform, and dichlorobenzene and hexamethyldisilane (HMDS).

5.2.2 Precursor Solution Preparation: 18 mg/ml PVA was weighted and dissolved in DI water overnight using a magnetic stirrer. For FTM processed OSC layer 10 mg/ml of DPP-DTT was dissolved using a magnetic stirrer in a solution made up of chloroform and dichlorobenzene in a fixed volume ratio (8:2) on a magnetic stirrer for 6h at 50°C [86]. To remove the undissolved or larger particles all the solutions were filtered using a PTFE based 0.22 µm syringe filter to get uniform film in solution processing.

5.2.3 Device Fabrication Steps:

The fabrication process involved dicing a heavily doped p-type silicon substrate (which was also used as the bottom gate electrode) into ~ 1.5 × 2 cm. Subsequently, the diced substrates were cleaned ultrasonically for 15 min in Acetone, Isopropyl alcohol, and rinsed with DI water. The cleaned and dried silicon substrates went under the plasma cleaning unit for 15 min to create a hydrophilic surface for better adherence of the dielectric film. Subsequently, the filtered PVA solution was spin-coated on the plasma-cleaned silicon substrates at 2500 rpm for 60 sec. The coated film was then baked at 80 °C for 5 minutes before heating at 100°C for 60 min. To prepare a floating film of DPP-DTT around ~15 µL of the prepared OSC solution was dropped over the water surface as depicted in Fig. 5.1 (g). The nice floating film of the DPP-DTT was obtained as shown in Fig 1(f). The obtained film was stamped on the PVA coated Silicon substrate and heated at 100 °C for 1.5 hours. For Source drain electrodes, gold

was evaporated thermally using Hind Hivac 1242D unit ($\sim 1 \times 10^{-6}$ Torr at ~ 0.04 nm/sec.) (with channel dimensions of $1000 \mu\text{m}/30 \mu\text{m}$) were deposited using metal masks (purchased from Ossila Ltd UK). Another control device with the same process was fabricated by making two changes firstly the PVA layer was crosslinked thermally by heating at 60°C for 10 hours and then using self-assembled monolayer (SAM) treatment over PVA (utilizing HMDS vapor treatment which again is known to passivate the surface trap charges [86]).

5.3 Characterization

5.3.1 AFM and Surface Morphologies of the Dielectric Film and Semiconducting Layer

In order to characterize the dielectric and OSC surface, the PVA film over the p^{++} silicon and water transferred DPP-DTT film over the PVA surface was analyzed using NTEGRA Prima from NDMDT Services Netherlands in tapping mode. The 2D/3D Atomic force microscopy of the PVA film as shown in Fig. 5.2 (a) and (b) shows a very smooth surface with root mean square roughness (R_q) of ~ 0.436 nm. The surface smoothness of this order is generally a required criterion for the satisfactory operation of OFETs. The DPP-DTT film over PVA shows film surface roughness of ~ 2.6 nm over an area of $\sim 5 \mu\text{m} \times 5 \mu\text{m}$ (2D/3D image included in Fig. 5.2 (c) and (d)). The thickness of the PVA dielectric layer was found to be ~ 25 nm while DPP-DTT thickness was $\sim 28 \pm 4$ nm utilizing Filmetrix FV 20.

5.3.2 UV Vis NIR analysis of DPP-DTT

UV-Vis NIR analysis of DPP-DTT Film (on Quartz substrate) transferred from water as liquid substrate was carried out using a Jasco 770 UV spectrophotometer. The FTM transferred DPP-DTT film has a broad spectrum ranging from 600 nm to 1000 nm with peak at ~ 821 nm which

is in good agreement with previous reports of DPP-DTT [58], [59]. Such features make DPP-DTT a suitable active material for NIR OPTs.

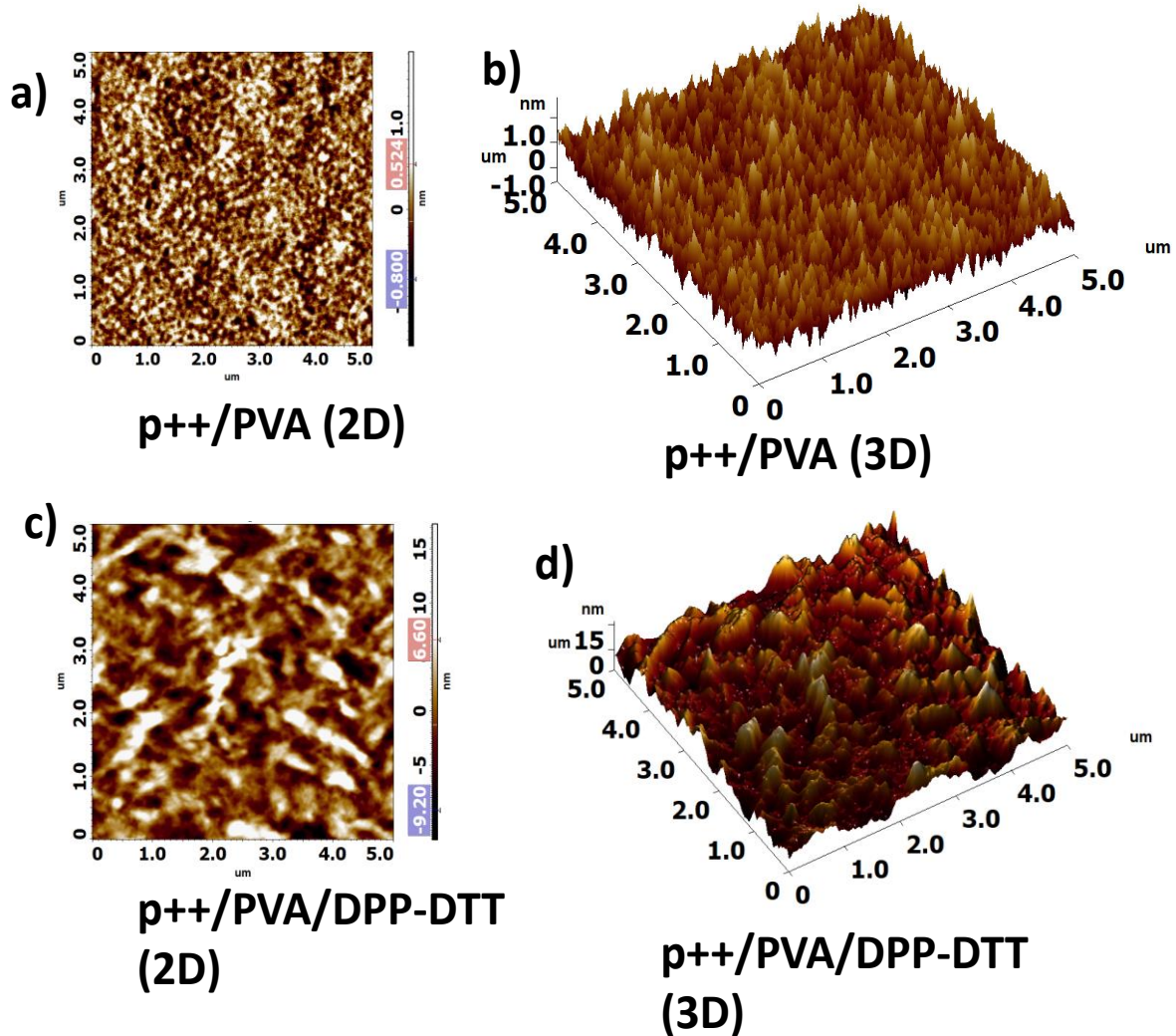


Fig. 5.2. (a) and (b) 2D,3D AFM images of PVA over p++ Si (c) and (d) 2D, 3D AFM images of FTM transferred DPP-DTT over PVA surface.

5.3.3 Dielectric Characterization In order to investigate the insulating properties of PVA dielectric metal insulator Semiconductor (MIS) structures were fabricated (under similar conditions) with gold top contacts. The leakage current behavior of the PVA film is shown in

Fig. 5.3 (b). The leakage current density is $\sim 1.9 \times 10^{-8}$ A/cm² at -1 V. The leakage current is in the same range as the earlier reported values of PVA film which are not crosslinked or passivated [123], [129]–[131]. Areal capacitance measurement of the same MIS structure was done using Agilent B1500A semiconductor parameter analyzer and is plotted in Fig 3 (a). The film thickness of coated PVA film was obtained as ~ 25 nm utilizing Filmetrix FV 20. Using this thickness and capacitance value at 1 KHz the effective dielectric constant of the PVA was calculated to be ~ 6.4 using parallel plate capacitor concept[132] which is in the same range as earlier reported values[123].

5.4 Results and Discussion

5.4.1 Electrical Characterization of OFETs

The dark and NIR light mode ($\lambda = 850$ nm, $I_{\max} = 1.2$ mW/cm²) characteristics of the unencapsulated PVA/DPP-DTT OFETs were measured using Agilent B1500A parameter analyzer. The dark mode transfer and output characteristics (as shown in Fig 5 (b) and (a)) of the DPP-DTT based OFET show a typical p-type behavior and saturation regime under V_{DS} and $V_{GS} = -1$ V. These devices are operating at ultra-low voltage of -1 V which is much smaller than all the devices compared in table 1. However current is extremely low which may be attributed to traps on the PVA surface (due to the high density of Hydroxyl groups) since the PVA surface is neither crosslinked nor any surface treatment for passivation of traps has been carried out[123]. Equations (5.1) and (5.2) have been used for the calculation of threshold voltage and mobility. The threshold voltage of -0.56 V, mobility of 0.082 cm² V⁻¹sec⁻¹, and the on-off ratio of $\sim 10^4$ were obtained for the device under dark mode. Fig. 5.5 (c) and (d) show the transfer curve of the PVA/DPP-DTT OFET on exposure to different intensities of light. All

the measurements and parameter extraction have been carried out using forward scan until or unless specified.

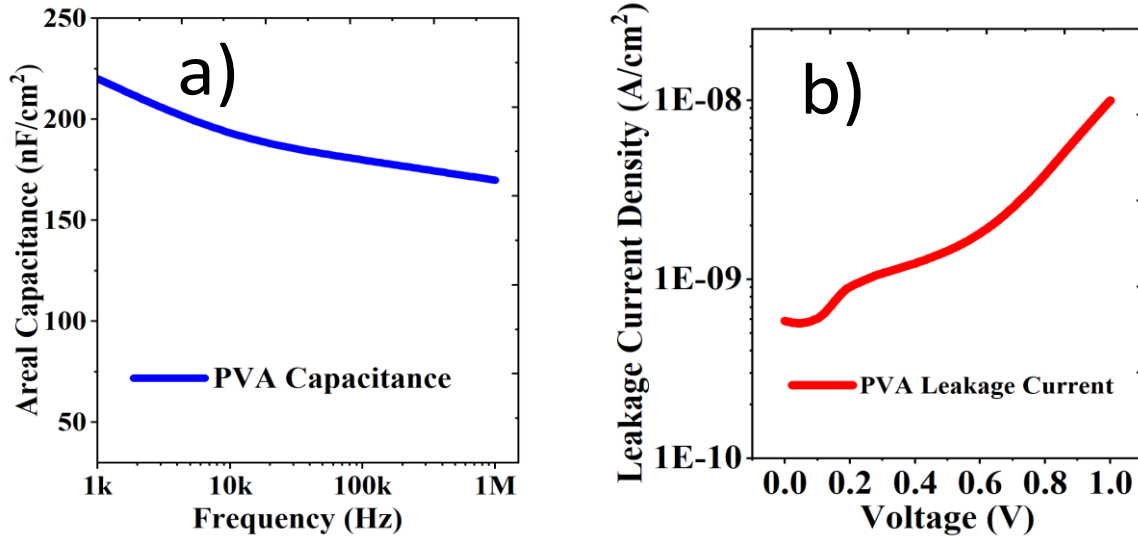


Fig. 5.3. (a) Areal capacitance and (b) Leakage current density of PVA

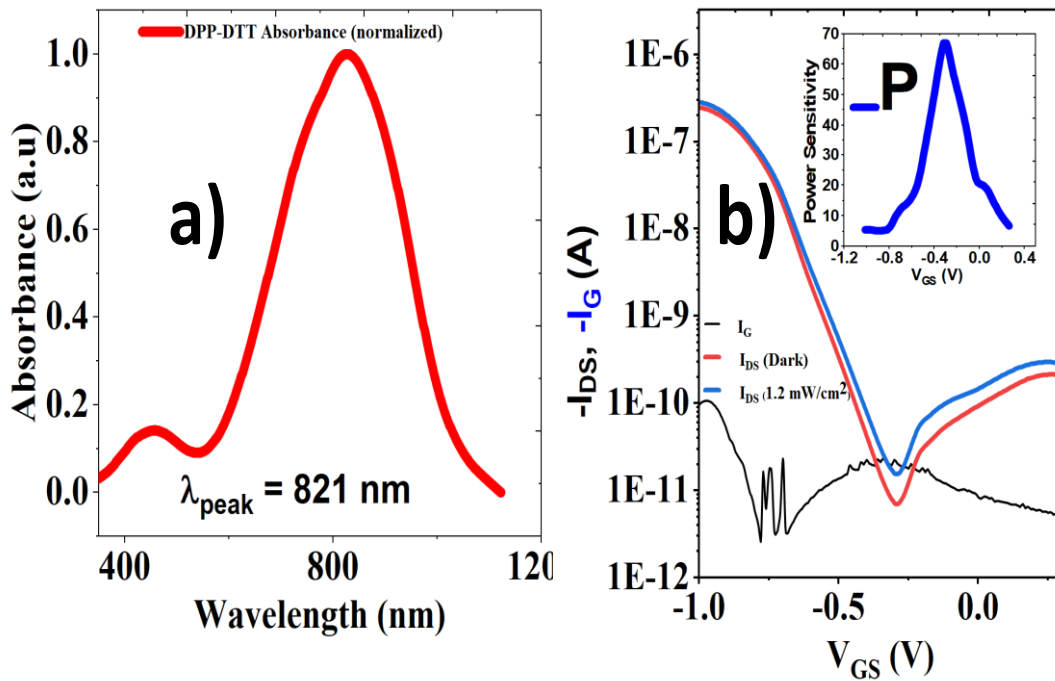


Fig. 5.4. (a) absorption spectrum of FTM transferred DPP-DTT (b) Negligible photo response of HMDS treated (Thermally crosslinked) PVA/DPP-DTT OFET.

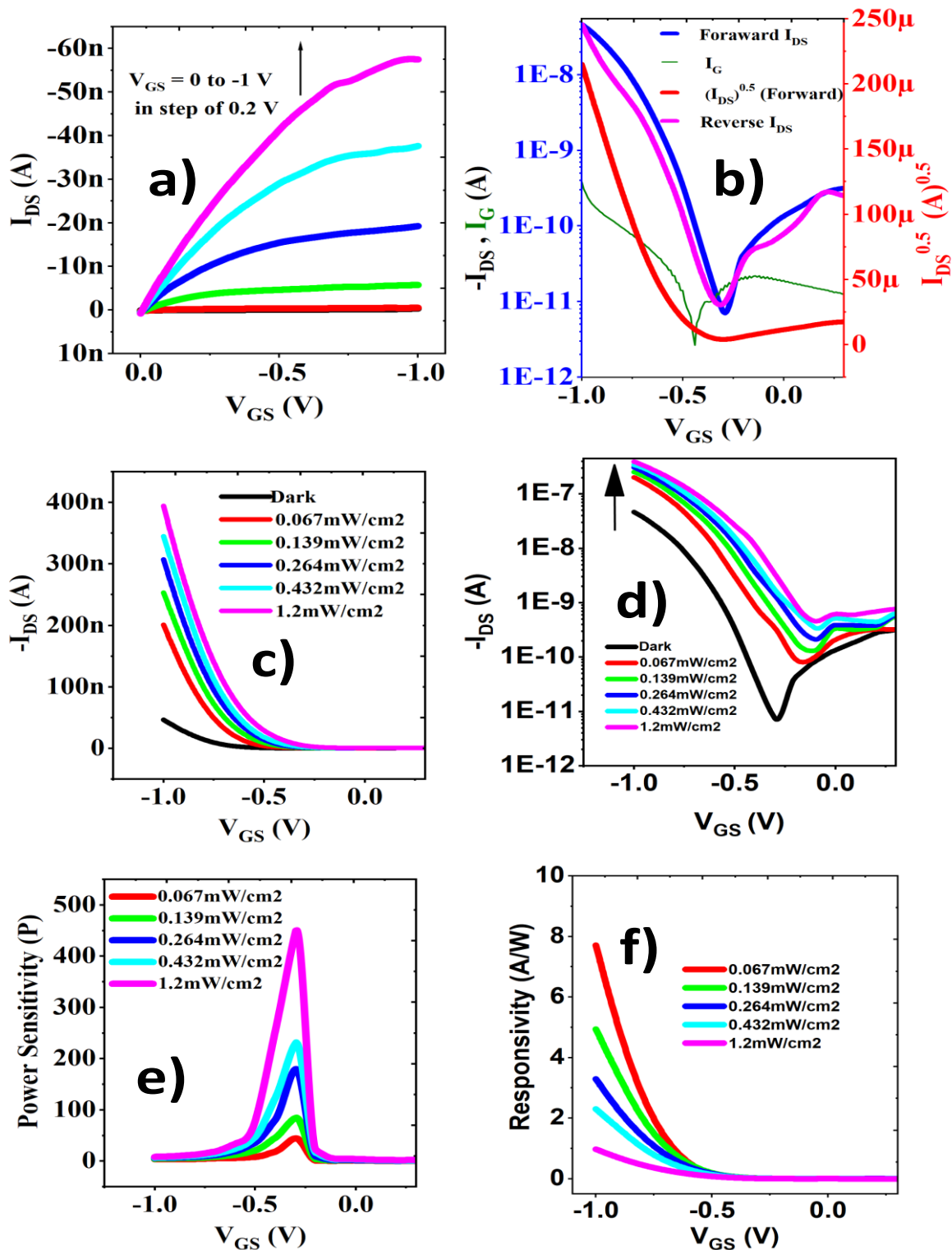


Fig. 5.5. (a) Output characteristics and (b) Transfer characteristics of PVA/ DPP-DTT OFET in the dark. (c) Transfer Characteristics of the OFET under NIR illumination (d) Semi-log Transfer Characteristics of the OFET under NIR illumination. (e) Power Sensitivity of OFET and (f) Responsivity of OFET at $V_{DS} = -1$ V.

5.4.2 OPT parameter Extraction and Discussion

On exposure to NIR light of increasing intensities ($\lambda = 850$ nm) the transfer curve (as shown in Fig. 5.5 (c) and (d)) shifts in the right direction with a net positive shift of threshold voltage (attributed to the Photovoltaic effect) and off current increases (due to the Photoconductive effect). The performance parameters such as photosensitivity (P), Responsivity (R), External Quantum efficiency (EQE), and detectivity (D) have been calculated using the formulas given by equations (5.3), (5.4), (5.5), and (5.6)[58]–[60], [120], [133].

$$I_D = \frac{\mu C_i W}{2L} (V_{GS} - V_{TH})^2 \quad (5.1)$$

$$\mu = \frac{2L}{W} \left(\frac{\partial I_D}{\partial V_{GS}} \right)^2 \quad (5.2)$$

$$P = \frac{I_{photo} - I_{dark}}{I_{dark}} \quad (5.3)$$

$$R = \frac{I_{photo} - I_{dark}}{AP_{in}} \quad (5.4)$$

$$EQE = \frac{Rhc}{\lambda} \quad (5.5)$$

$$D = \frac{R\sqrt{A}}{\sqrt{2qI_{dark}}} \quad (5.6)$$

Where C_i , I_D , V_{GS} , q , W , L , and kT I_{photo} , I_{dark} represents capacitance per unit area of the gate dielectric, drain current, gate-source voltage, the charge on an electron, channel width, channel length, thermal energy, photocurrent, and dark respectively.

Using the transfer curve in Fig. 5.5(d) the photosensitivity (P) and responsivity (R) have been plotted with variation in gate voltage and various intensities in Fig 5 (e) and (f) respectively.

The photosensitivity shows a maximum value of 456 at $V_{GS} = -0.3$ V and Intensity of 1.2 mW/cm^2 while responsivity is maximum at $V_{GS} = -1$ V, $V_{DS} = -1$ V, and intensity of 0.067 mW/cm^2 . The photosensitivity is maximum in the neighborhood of threshold voltage when the device is in the off state. This can be explained by the fact that net current in an illuminated device is due to photogenerated carriers and field effect. Thus, in the off-state the photogenerated current dominates over the field effect current. However, at higher voltages the field effect current dominates over photocurrent thus photosensitivity falls when the device is in on state. This behavior of PVA/DPP-DTT is consistent with previous reports of OPTs[60]–[62], [120]. Fig 6 (a), (b), and (c) represents Responsivity, Detectivity, and EQE on variation in illumination intensity. The device exhibits a Responsivity of ~ 7.72 A/W, Detectivity of $\sim 1.097 \times 10^{12}$ Jones, and EQE of ~ 1183.84 % at $0.67 mW/cm^2$ at $V_{GS} = V_{DS} = -1$ V. The EQE value greater 100 % can be explained by the photomultiplication phenomenon arising due to the trapped electrons at the dielectric organic semiconductor interface which reduces the hole injection barrier (explained in detail in next section).[59] The fitted value of R, D, and EQE shows sublinear dependence ($R \sim I^{-0.72}$) with intensity which is in accordance with earlier reports[56], [58], [59]. The sublinear behavior is generally attributed to the saturation phenomenon of photogenerated charge carriers in the channel on increasing the intensity. A variation in threshold voltage shift and change in trap density (Δn) using formula $\Delta n = \frac{\Delta V_{TH} C_i}{q}$ [44] with respect to increased intensity of NIR light has been plotted in Fig. 5.6 (d). Percentage change in mobility (with actual values in bracket) has been represented in Fig. 5.7 (a).

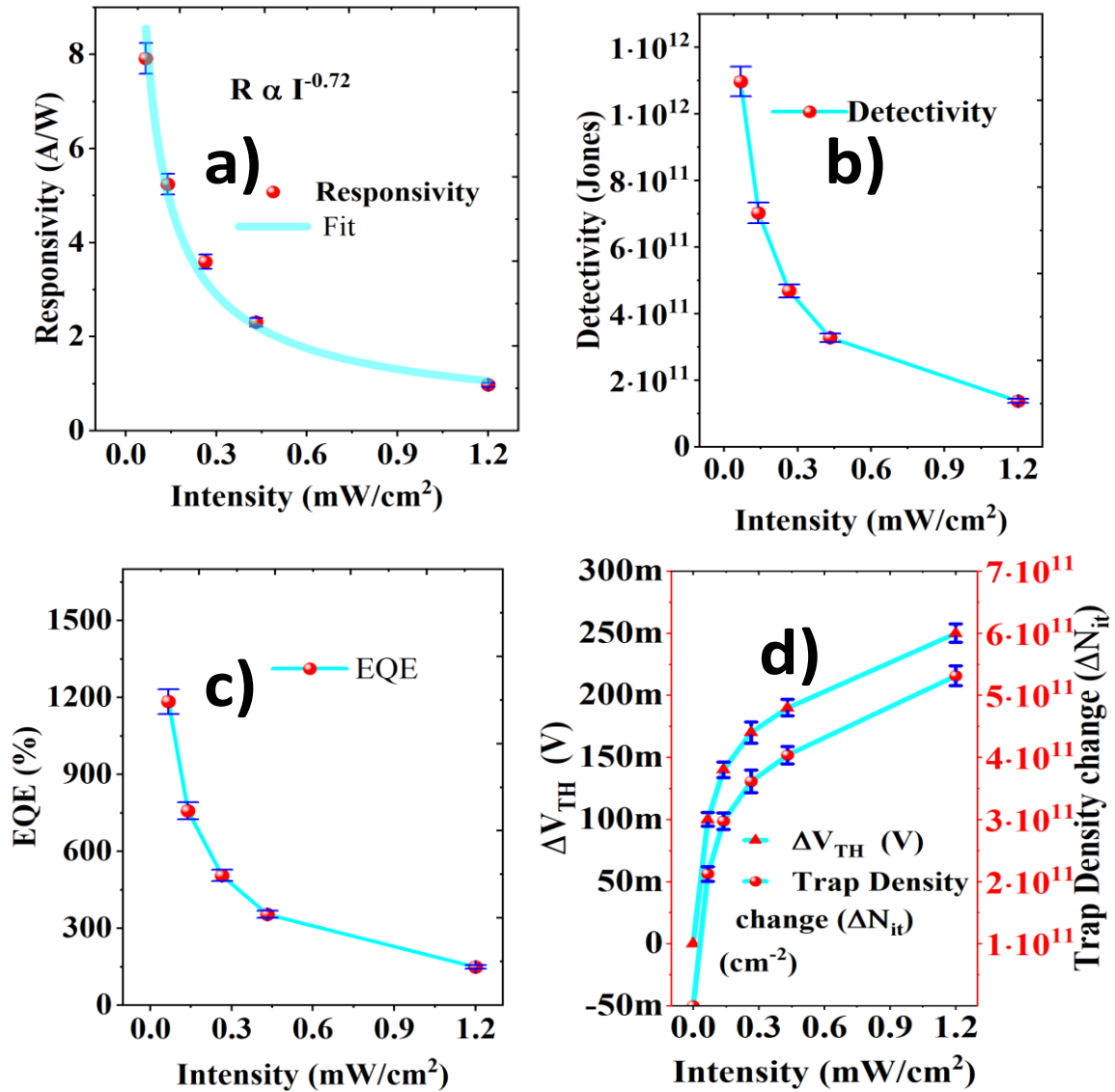


Fig. 5.6. (a) Responsivity (b) Detectivity, (c) EQE, and (d) Threshold Voltage Shift and trap density change of PVA/DPP-DTT OFET on varying Intensity at VGS = VDS = -1 V.

5.4.3 General Working and Mechanism of Performance Enhancement of OPT

In OPTs there are two phenomena that govern the photocurrent mechanism on illumination with light namely photovoltaic and photocurrent. The photovoltaic mechanism is dominant when OPT is in on state. Illumination of light on DPP-DTT film results in exciton generation

which later separates into free electrons and holes. While the holes move towards the drain the electrons get trapped by hydroxyl ions at OSC/ PVA interface. These trapped electrons get accumulated under the source electrode and effectively reduce the hole injection barrier thereby decreasing the threshold voltage (Right shift of the threshold voltage) and increasing the I_{DS} . This is the photovoltaic mode which shows the logarithmic dependence of the drain current with increasing intensity of light. The photon current in this mode is given by equation (5.7) while for photoconductive mode it is represented by equation (5.8) [58], [59], [61] where A and B are fitting parameters hc/λ is the photon energy, P_{in} is the input power, η is the quantum efficiency, and I_{ph} is photon current.

$$I_{ph} = A \frac{kT}{q} \ln\left(1 + \frac{q\eta\lambda P_{in}}{hcI_{dark}}\right) \quad (5.7)$$

$$I_{ph} = BP_{in} \quad (5.8)$$

The photon current in the ON state ($V_{GS} = -1$ V and $V_{DS} = -1$ V) and in the OFF state ($V_{GS} = -0.3$ V and $V_{DS} = -1$ V) as a function of incident power (P_{in}) has been plotted in Fig. 5.7 (c) and (d). The experimental data has been shown in black dots which has been theoretically fitted using equation (5.7) and (5.8) using logarithmic and linear function. The clear logarithm fit of I_{DS} versus Intensity (as shown in Fig. 5.7 (c)) in on-state and linear fit of I_{DS} in off-state (as depicted in Fig.5.7(d)) provides compelling evidence that the photogeneration mechanism in PVA/DPP-DTT OFETs is governed by photovoltaic and photoconductive effect as discussed before. As shown in Fig. 5.7 (a) Charge carrier mobility of DPP-DTT OFET increased by more than 300% on illumination with increased intensity of radiation. This may be again attributed to poor charge carrier transport arising due to charge traps (high density of hydroxyl groups)

on the PVA surface. Due to these traps at the semiconductor/dielectric interface, the mobility of OFET is poor under a dark environment despite the smooth polymer dielectric surface of PVA ($R_q \sim 0.436$ nm from Fig. 5.2 (a) and (b)). On exposure to light of different intensities, the photogenerated electrons get trapped by these hydroxyl ions thereby decreasing the hole injection barrier at the source electrode leading to increased mobility. It is worth noting that DPP-DTT has the tendency to show higher mobilities[134]. Finally, such good performance of PVA/DPP-DTT NIR OPT can be explained using the concept of charge trapping at the dielectric/semiconductor interface. The hydroxyl ions on the PVA surface help in performance improvement in two ways. Firstly, it results in a very low dark current (by limiting the charge carrier transport), and secondly on illumination these charge traps (hydroxyl ions) act as electron trapping center and traps the photogenerated electrons resulting in the accumulation of electrons at the PVA/OSC interface which further reduces the hole injection barrier. Due to the reduction of the hole injection barrier hole mobility increases (This is supported by an increase in mobility on illumination as shown in Fig.5.7 (a)). Additionally, an increase in mobility on illumination results in efficient exciton dissociation and separation. The fabricated device with HMDS vapor-treated (and thermally crosslinked) PVA film shows a very small change in photocurrent which further confirms that the performance improvement is due to the interfacial traps available on untreated PVA surface. The small change in drain current on illumination and corresponding photosensitivity of HMDS-treated and thermally crosslinked PVA-based OFET is shown in Fig. 5.4(b). This is because the polar hydroxyl groups on the surface of PVA has been passivated by HMDS treatment and thermally crosslinking so the device shows a low photosensitivity of ~ 70 which is consistent with earlier reports where passivated trap based devices showed negligible photoresponse[126] The presence of small

hysteresis (as shown in Fig. 5.5(b)) in the unpassivated PVA based device further confirms the presence of surface charge traps while HMDS treated device shows no hysteresis confirming effective passivation of trap charges at the dielectric-semiconductor interface. This further validates that performance enhancement is due to surface charge traps.

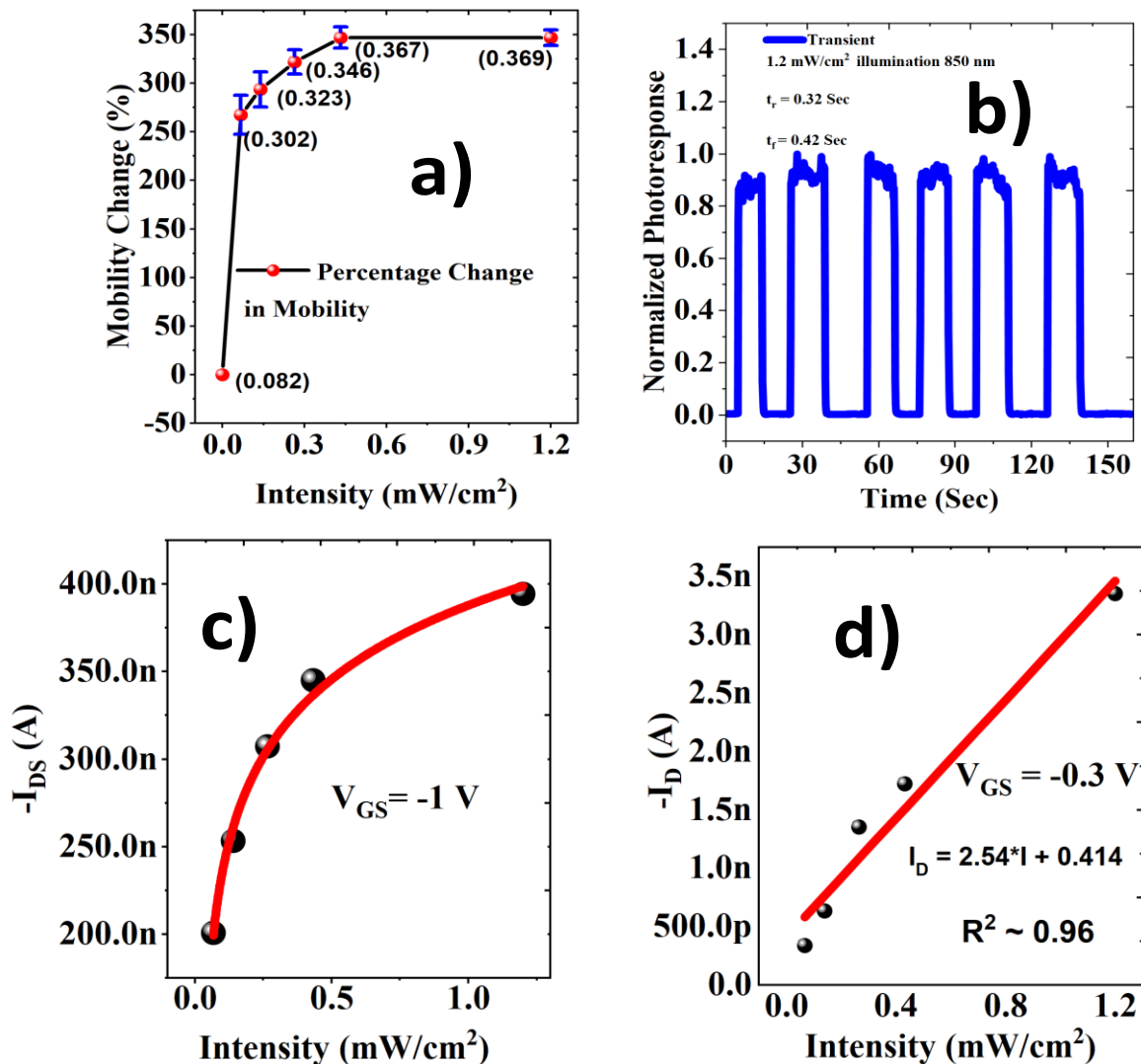


Fig. 5.7. (a) Mobility variation with values of exact mobility in bracket (unit - $\text{cm}^2 \text{V}^{-1}\text{sec}^{-1}$), (b) photoswitching of PVA/DPP-DTT/OFET at $V_{GS} = V_{DS} = -1$ V and 1.2mW/cm^2 (c) Drain current variation at $V_{GS} = V_{DS} = -1$ V (On state) with logarithmic fit (Photovoltaic Mode) and (d) Drain current variation at $V_{GS} = -0.3$ V and $V_{DS} = -1$ V (OFF state) with the linear fit (photoconductive Mode) with different intensities of NIR light.

TABLE 5.1

COMPARISON OF PRESENT WORK WITH EXISTING REPORTED OPT

| Structure | R_{\max} (A/W) | P_{\max} | I (mW/c m ²) | λ (nm) | Deposition method (OSC/Dielectric) | V_{DS}/V_{GS} (V) | Ref. |
|---|---------------------|--------------------|--------------------------------|-------------------|--|------------------------|--------------|
| SiO ₂ /PBIBDF-TT | 0.44 | 3.3×10^4 | 47.4 | 808 | PDMS Template/NA | 80 | [58] |
| SiO ₂ /DPP-DTT (Nano-Wires) | 246 | 10^3 | 14.47 | 850 | SC/NA | -30 | [59] |
| PMMA/ PODTPPPD- BT/PMMA/P3HT | 0.021 | 26.1 | 4.25 | 905 | SC/SC | -30/-30 | [62] |
| HfO ₂ /PVP/TIPS | 0.011 | 40 | 0.3 | 620 | SC/V/SC | -5/-10 | [120] |
| AlO _x /ODPA/DPP- DTT | 0.10 | 2.54×10^4 | 48.40 | 808 | SC/SC | -5 V /-5 V | [135] |
| PMMA/P3HT/PbS CQDs | 0.0094 | 947 | 200 | 980 | SC | -10/-40 | [61] |
| PVA/DPP-DTT | 7.98 | 4.56×10^2 | 1.2 | 850 | W-FTM/SC | -1/-1 | This Work |

5.4.4 Transient Analysis of OPTs

Fig 5.7 (b) shows the photoswitching behavior of PVA/DPP-DTT at $V_{DS} = V_{GS} = -1$ V and intensity of 1.2 mW/cm^2 with a rise and fall time of 0.32 sec and 0.42 sec respectively. Six on-off cycles of the device show the stability and repeatability of the fabricated device. The transient time response which includes rise time (t_r) and fall time (t_f) has been calculated using the 10% to 90 % and 90 % to 10 % concept [58], [59], [61].

5.4.5 Comparative Analysis with Existing works

Table 5.1 compares the reported OPTs and their performance parameters along with the voltage of operation, maximum intensity used, and fabrication process used. In Table 5.1 SC refers to spin coating, V stands for vapor deposition technique, and W-FTM stands for Floating film transfer method from the surface of water as substrate. The majority of compared devices are working at very high voltage making them unsuitable for portable sensors. Additionally, for the OSC layer, the used method in compared devices is Spin coating or template based which is unsuitable for large-area electronics. Furthermore, this work is more suitable and easily adaptable to flexible and wearable electronics as it has utilized water processed PVA as polymer dielectric with a maximum processing temperature of 100°C .

5.5 Conclusion

In Summary, this report demonstrates an ultra-low voltage NIR OPT with PVA dielectric layer and FTM transferred DPP-DTT OSC film. The device showed responsivity of 7.72 A/W , photosensitivity of 456, EQE of 1183.84 %, and detectivity of 1.097×10^{12} Jones all under -1 V operation. The logarithmic and linear fit of the drain current in on-state and off-state with

the experimental data respectively confirm the photovoltaic and photoconductive modes of operation of the device. Such high performance of NIR OPT can be explained with the help of the charge trapping effect due to the presence of hydroxyl ions on the PVA dielectric surface which results in a very low dark current and reduced hole injection barrier due to electron trapping by hydroxyl ions on illumination. This has been further confirmed by fabricating another device in which charge traps on the PVA layer have been passivated by thermal crosslinking and using HMDS treatment. The thermally crosslinked and HMDS-treated device shows a very small change in the current on illumination. The maximum processing temperature of 100°C for both the dielectric layer and OSC and FTM transfer method adapted for OSC makes this device suitable for future applications in flexible and large-area electronics. Furthermore, since this report utilizes Water as FTM substrate for OSC layer transfer and for PVA dielectric processing, makes it an eco-friendly suitable processing of NIR OPTs.

